International Journal of Science and Engineering Invention (IJSEI)
Volume 09, August 2023,
https://doi.org/10.23958/ijsei/vol09-i08/250

Original article

Zonal Estimation of Paddy Straw Based Bioenergy Potential using Landsat 8 OLI Satellite Imagery

Hemant Sahu *, Pushpraj Singh

Department of Rural Technology and Social Development, Guru Ghasidas Vishwavidyalaya Bilaspur Chhattisgarh, India

*Correspondence author: Hemant Sahu; *info2hemant1980@gmail.com*

Received 22 May 2023; Accepted 28 July 2023; Published 05 August 2023

Abstract

Paddy (Oryza Sativa L.) is one of the important crops not only in India but also in the world, it is vital to determine the paddy field and its residues viz. paddy straw as accurately as possible using fast and economical methods such as remote sensing and GIS to support bioenergy potential. Accurate and timely paddy field maps with a fine spatial resolution would greatly improve our understanding of the effects of paddy on food and water as well as energy security. In this study, special mapping algorithm that uses NDVI time series data derived from Landsat 8 OLI imagery developed to identify paddy fields and area to estimate the paddy crop residue potential and agriculture-based bioenergy potential in the study area. The results validated with ground field works data at 60 well-distributed sample points. It was found to be 25102.89 hectares in Kharif and 14527.89 hectares in Rabi season. Among all, Khishora and Hasda were having annual paddy straw potential of more than 1800 tonnes. Hasda and Khishora was having maximum paddy straw based bioenergy potential with more than 27000 GJ whereas Kewradih shows the maximum paddy straw based bioenergy potential of 101 GJ per households per annum and 20 GJ per capita per annum. The overall accuracy of the method was 74.0 % and kappa coefficient was 0.80.

Keywords: ***Paddy Straw Potential, Landsat 8 OLI, Zonal Estimation, Bioenergy Potential.***

1.0 Introduction

Energy is one of the major drivers of development as well as access to clean, safe and affordable sources [26]. It can stimulate economic, social and physical development leading to critical improvement in people's livelihood. The availability of reliable and cheaper energy is essential for economic development. Reliable access to energy may be a basic precondition for up people's lives in rural areas that increased healthcare, education and growth among native economies. Nearly 80 per cent of this population resides on rural areas; most have scant prospects of gaining access to electricity within the coming future [19]. The satellite imagery using passive (optical) sensors and active (radar and LIDAR) are often used effectively in estimating biomass, series of SHP, and find the potential areas for solar energy, hydro power, geo-thermal and wind energy. Remote sensing facilitate to analysis the land use pattern, elevation, catchment basin, soil classification, stream network, flow characteristics, existing parcel of land, and variety of attributes for appropriate site selection to develop the hydropower. The remote sensing and GIS as a decision-making tool, has expedited combining evaluations of environmental, social and political constraints with engineering decision to provide the best decision support system [02]. Remote sensing is being used either within the estimation of biomass potential, accessibility and practicability for production and site selection of the power plants and therefore the biomass plantation, nearest to the grid line and biomass transportation cost on the basis of the amount of biomass and transportation distance [17].

Agrarian fields are developed and managed through a variety of social conduct or programs, which can monstrously impact biogeochemical and hydrologic cycles, climate, ecosystem functions, the frugality and mortal health [32]. Thus, mapping crop are to carry out social programs as well as estimating the quantum and type of crops gathered in a certain area. The Landsat series data are suitable for land characterisation conditioning, owing in large part to the spatial, spectral and radiometric rates of the data [33,31]. The data acquired from Landsat satellites are also useful for assessing the condition of foliage. Status of vegetation can be calculated from simple formulas that correspond of a combination of two or further reflectance wavebands calculated from colourful satellite data. Specifically, the Normalized Difference Vegetation Index (NDVI), calculated from Landsat data, has been applied for covering foliage systems or ecological responses to environmental change [10]. Vegetation also presents precious information for understanding the natural and man- made surroundings through quantifying foliage cover from original to global scales at a given time point or over a nonstop period. It's critical to gain current countries of foliage cover in order to initiate foliage protection and restoration programs [06]. At the global and indigenous scales, several early studies of ecosystems and land cover have involved mapping paddy rice fields grounded on agrarian tale data. In the late 1980s and early 1990s, several paddy rice datasets with coarse spatial resolution were produced to assay global climate and hothouse gas emigration [21,01]. In recent years, various studies were conducted on paddy crop by using agrarian data at large scale [08,29]. Although most of satellite datasets were of coarse resolution from multiple sensors. Satellite remote sensing has been extensively applied and has been recognised as a powerful and effective instrument in detecting land use and land cover changes [22]. A number of studies have explored

the eventuality of satellite images for analysis vegetation changes. Optical remote sensing were frequently used to map rice crop phenology and cropping schedule. Several studies on the remote sensing based assessment for the potentiality of energy resources along with the prototype of energy utilization in rural vicinity have been carried throughout the globe including India. Still much remains to be done at local needs. The present study site i.e., rural areas of Magarlod block of Dhamtari district is sufficient in order to the availability of energy resources which provides a great possibility and potentiality for sustaining the energy demand of existing rural communities.

The studies on assessment of energy resources through the application of remote sensing and GIS from different areas of Chhattisgarh has been limited and altogether absent in rural areas of Magarlod block of Dhamtari district. Therefore, it was planned to investigate the distribution and availability of paddy crop and straw resources potential, way of energy consumption in locality of rural areas and generate an appropriate course of action for sustainable energy security in rural areas of Magarlod block. Thus an attempt was done to find paddy cropping pattern dynamics and straw potential using time series Landsat 8 OLI data in study area.

2.0 Materials and Methodology

2.1. Study area

Magarlod is a Block situated in Dhamtari district in Chhattisgarh. Positioned in rural region of Chhattisgarh, it is one among the 4 blocks of Dhamtari district. As per the administration register, the block code of Magarlod is 113. The block has 116 villages and there are total 24884 houses in this Block. Population of Magarlod Block: As per Census 2011, Magarlod's population is 115150. Out of this, 57387 are males whereas the females count 57763 here. This block has 15707 kids in the age bracket of 0-6 years. Out of this 7917 are boys and 7790 are girls. Literacy rate of Magarlod Block: Literacy rate in Magarlod block is 65%. 74949 out of total 115150 populations are educated here. Among males the literacy rate is 73% as 42315 males out of total 57387 are educated while female literacy rate is 56% as 32634 out of total 57763 females are educated in this Block. The illiteracy rate of Magarlod block is 34%. Here 40201 out of total 115150 people are illiterate. Male illiteracy rate here is 26% as 15072 males out of total 57387 are uneducated. In females the illiteracy rate is 43% and 25129 out of total 57763 females are illiterate in this block. Agricultural status of Magarlod Block: The count of employed people of Magarlod block is 59896 however 55254 are un-employed. And out of 59896 working people 17125 persons are completely dependent on farming.

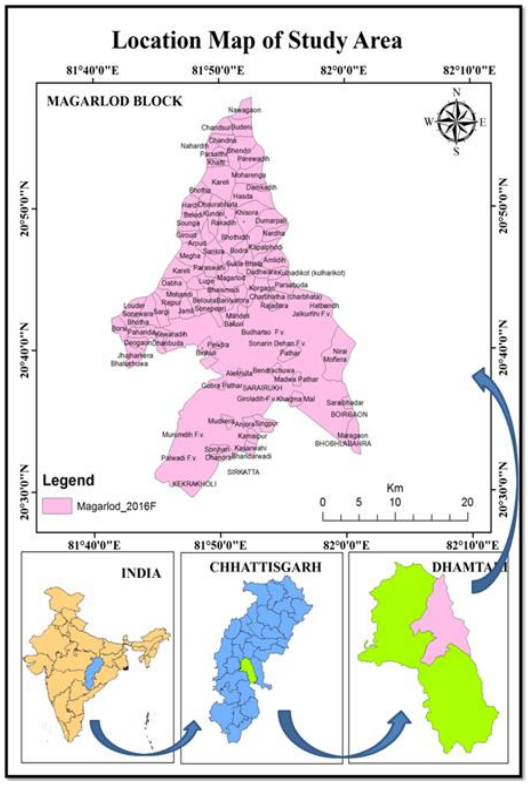

Insert Figure 1: Location Map of Study Area

2.2. GIS Data

Geographical Information data act as an important support system for the location specific decision and planning. It provides us ground information to maximum possible accuracy within the available resources. Vector data or village boundary was an important input data required for the limiting the boundary of study. It can be drawn through using the topo-sheet provided by the authorized agency that was Survey of India coded with individual number system for every sheet.

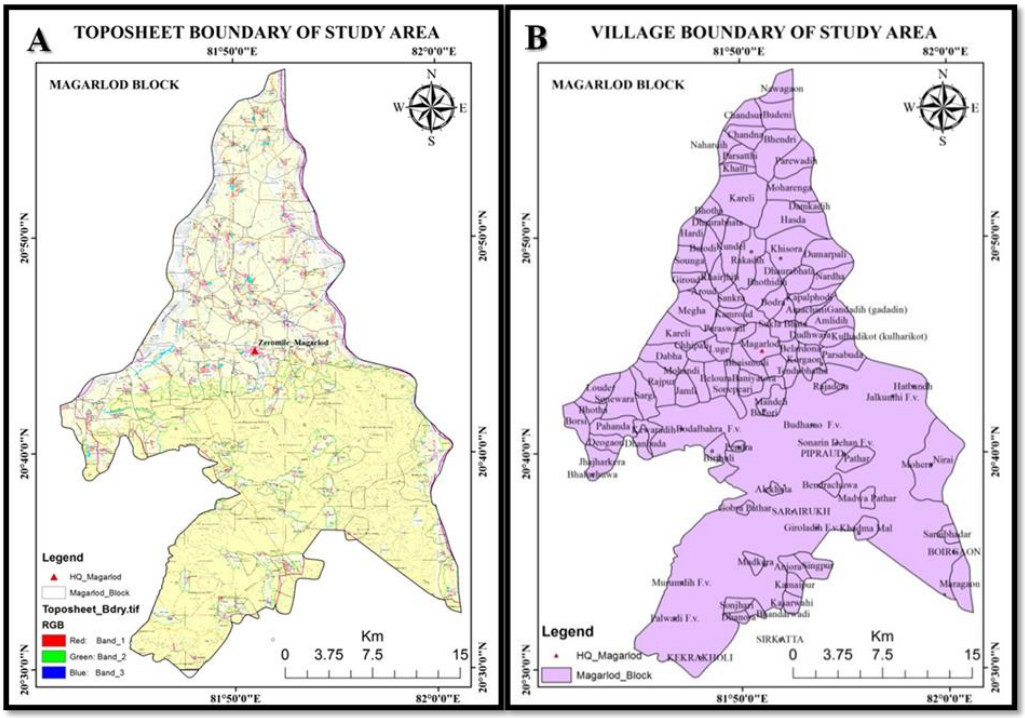

Insert Figure 2: Toposheet Map (A) and Village Boundary (B) of Study Area

The toposheet used for the study was No 64/H/10, 64/H/13, 64/H/14 and 64/L/2 procured from Survey of India and village boundary of Magarlod block of study area (**Figure 2**).

2.3. Satellite Imagery Data

Landsat 8 Operational Land Imager (OLI) is an American Earth observation satellite launched on 11 February 2013, a NASA and USGS collaboration, acquires global moderate resolution measurement of the earth's terrestrial and polar region in the visible, near infrared, short wave and thermal infrared [25]. For the present study Landsat 8 OLI satellite images with 11 spectral bands were used (**Figure 3**). Landsat 8 OLI Satellite Imagery bands spatial resolution varies from 15 meters for panchromatic to 100 meters for thermal band. Rest of bands is having spatial resolution of 30 meters for band from 1 to 7 and 9. The scene swath is 170 Km X 183 Km and the temporal resolution of the imagery is 16 days.

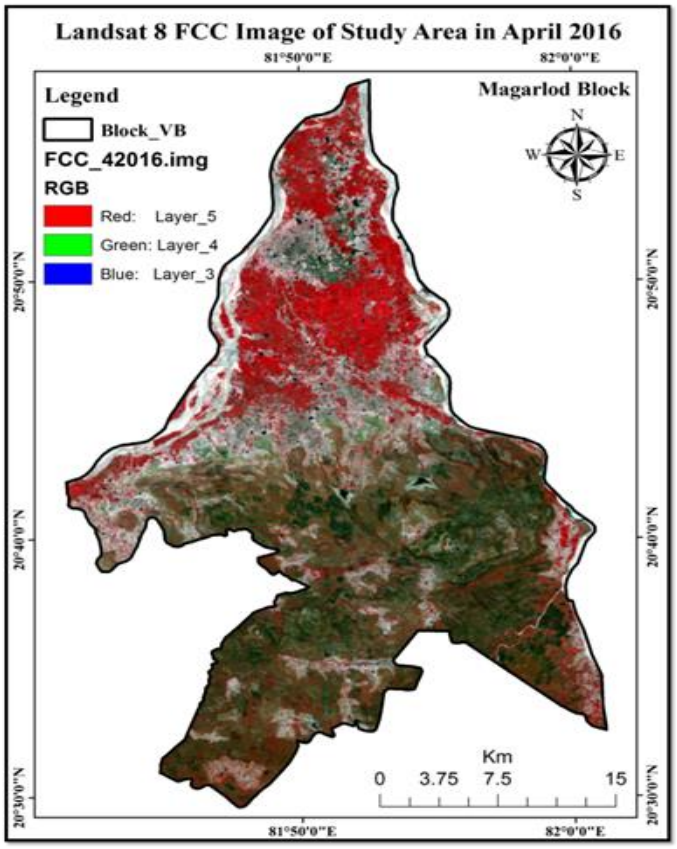

Insert Figure 3: False Colour Composite (FCC) Satellite Image of Study Area

Technical details of Landsat 8 OLI satellite imagery used for analysis were shown in table (Insert Table 1).

Insert Table 1: Band Specifications of Landsat 8 OLI Satellite Imagery [14]

S. No	Bands	Wavelength (micrometers)	Resolution (meters)
1	Band 1 - Ultra Blue (coastal/aerosol)	0.435 - 0.451	30
2	Band 2 – Blue	0.452 - 0.512	30
3	Band 3 – Green	0.533 - 0.590	30
4	Band 4 – Red	0.636 - 0.673	30
5	Band 5 - Near Infrared (NIR)	0.851 - 0.879	30
6	Band 6 - Shortwave Infrared (SWIR) 1	1.566 - 1.651	30
7	Band 7 - Shortwave Infrared (SWIR) 2	2.107 - 2.294	30
8	Band 8 – Panchromatic	0.503 - 0.676	15
9	Band 9 – Cirrus	1.363 - 1.384	30
10	Band 10 - Thermal Infrared (TIRS) 1	10.60 - 11.19	100 * (30)
11	Band 11 - Thermal Infrared (TIRS) 2	11.50 - 12.51	100 * (30)

2.4. Selection of Image Processing and Analysis Software

In the present study, ARC-GIS 9.3 license version software was used for the calculating and analysis of images. ARC-GIS are a programme that allows anyone to create maps by combining data with a shape file. Maps created with the program, can be edited in many ways and allowing to make maps that highlight specific information. The ARC-GIS provide different functionalities for calculating raster and vector data of any images along with Arc toolbars.

2.5. Selection of Satellite Data

Freely available temporal data of Landsat 8 OLI satellite imagery was downloaded from UGSG Earth Explorer [14]. Three different series for the year 2013, 2014, 2015 and 2016 were used for the month of Oct-Nov (Kharif), April (Rabi) and May (Zaid/Summer). Months of satellite acquisition was selected depending on availability of clear sky and cloud free satellite images as well as peak physiology condition of Kharif and Rabi paddy crops data analysis for agriculture biomass based potential energy estimation over the year, whereas month of May was selected due to most dry spell and least vegetation condition for the analysis of minimum forest based.

Insert Table 2: Acquisition Date and Parameters of Landsat 8 OLI Satellite Imagery.

S. No	Row	Path	Date of Image Capturing	Elevation Angle	Sin of Sun Elevation Angle	Multiplicative Value	Additive Value
	Kharif						
1	142	46	09-11-2013	48.38	0.7475534845	0.00002	-0.1
2	142	46	14-10-2015	55.35	0.8226622444	0.00002	-0.1
3	142	46	16-10-2016	54.64	0.8154933286	0.00002	-0.1
	Rabi						
4	142	46	02-04-2014	61.52	0.8789802100	0.00002	-0.1
5	142	46	05-04-2015	62.11	0.8838386750	0.00002	-0.1
6	142	46	23-04-2016	66.19	0.9148735593	0.00002	-0.1

Biomass area calculation to avoid any over estimation of potential energy. In this case available images for Kharif season was November 2013, October 2015 & October 2016, whereas for Rabi season was April 2014, April 2015 & April 2016. Similarly for forest biomass May 2013, May 2014, May 2015 and May 2016 images were used. For the study purpose Landsat 8 OLI images of different years were used for identifying of vegetation area, because the OLI images contains the eleven bands with different ranges and out of these 11 bands only two bands NIR and Red were used (**Table 2**).

2.6. Imagery Pre-processing and Analysis Tools

Pre-processing is an important step to minimize the presence of noise in any satellite imagery for any classification and object identification [07]. The most common steps involves in pre-processing are radiometric corrections followed by geo-rectification taking toposheet as base map. Further the images were clipped to the extent of study area using vector shape file provided by the Survey of India. The process was performed for all the scene of Landsat 8 satellite images in image processing software.

2.7. NDVI Analysis

Vegetation indices help to identify the distribution of vegetation and soil on the basis of reflectance behaviour of green vegetation. The NDVI is a simple ratio between near infra red and red band of optical imagery that can be used to assess whether the object being contains live green vegetation or not. Normalized Difference Vegetation Index (NDVI) was calculated as for using following equation as:

$$\mathbf{NDVI} = \frac{(\mathbf{NIR\ Band - RED\ Band})}{(\mathbf{NIR\ Band + RED\ Band})} \text{.....Eq.1}$$

Where (-1 < NDVI > +1)

Here RED is visible red reflectance, and NIR is near infrared reflectance. The wavelength range of NIR band is (0.851 - 0.879 µm) and Red band is (0.636 - 0.673 µm) in Landsat 8 OLI Satellite Imagery. The NDVI is larger for greater chlorophyll density towards positive side of range and is lower towards zero for less vegetation conditions. Negative value of NDVI indicates water, urban and other land use land cover without vegetation. It takes the (NIR - red) difference and normalizes it to balance out the effects of uneven illumination such as shadows of clouds or hills [30]. The NDVI for *Kharif* and *Rabi* season for agriculture residues estimation as well as in the month of May for forest biomass was calculated using equation 1 for each of the studied scene. In the next step mean NDVI for *Kharif* was calculated using raster calculation tool in ARC-GIS.

$$\mathbf{NDVI_{mean}} = \frac{\mathbf{1}}{\boldsymbol{n}} \sum_{\boldsymbol{i=1}}^{\boldsymbol{n}} \mathbf{NDVI}\boldsymbol{i} \text{ .....Eq. 2}$$

Where

$NDVI_{mean}$ = Mean NDVI of temporal imagery NDVI.
i = ($NDVI_1$, $NDVI_2$,.$NDVI_n$)
n = NDVI image of each individual studied scene for the year of 2013, 2015 and 2016.

The process was repeated for *Rabi* season with the NDVI year of 2014, 2015 and 2016. The mean NDVI for both the seasons was subjected to preliminary classification into six major land use land cover classes water body, dry river, settlement, uncultivated land, forest and agriculture (paddy crop).

2.8. Ground Truthing

Mean NDVI value of each classes were noted down and ten ground truthing points per classes were obtained in both the season, when satellite was passed in Rabi and Kharif season in 2016 with respective months. In this way, from six major classes namely; agriculture (paddy crop), forest, waterbody, urban settlements, dry river, and uncultivated land, nearly 51 ground truthing points were covered for *Rabi* season and similarly 60 points were covered for *Kharif* season using GPS. (**Figure 4A & 4B**).

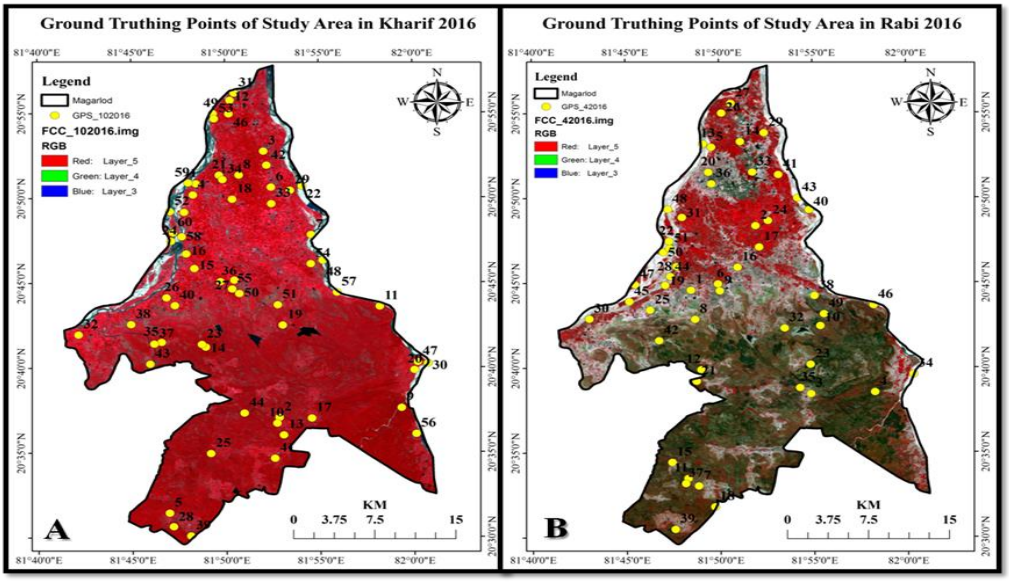

Insert Figure 4: Ground Truth Points in Kharif (A) and Rabi (B) Season in Study Area

2.9. Class Extraction and Acreage Estimation of Agriculture Residues:

After accuracy assessment NDVI images were reclassified into six classes to estimate the acreage estimation of each class in Rabi season as well as Kharif season. Again this reclassified image was used for extraction of Rabi season paddy crops as well as Kharif season paddy acreage by assigning a single value as 01 for crop and rest as No Data in the study area.

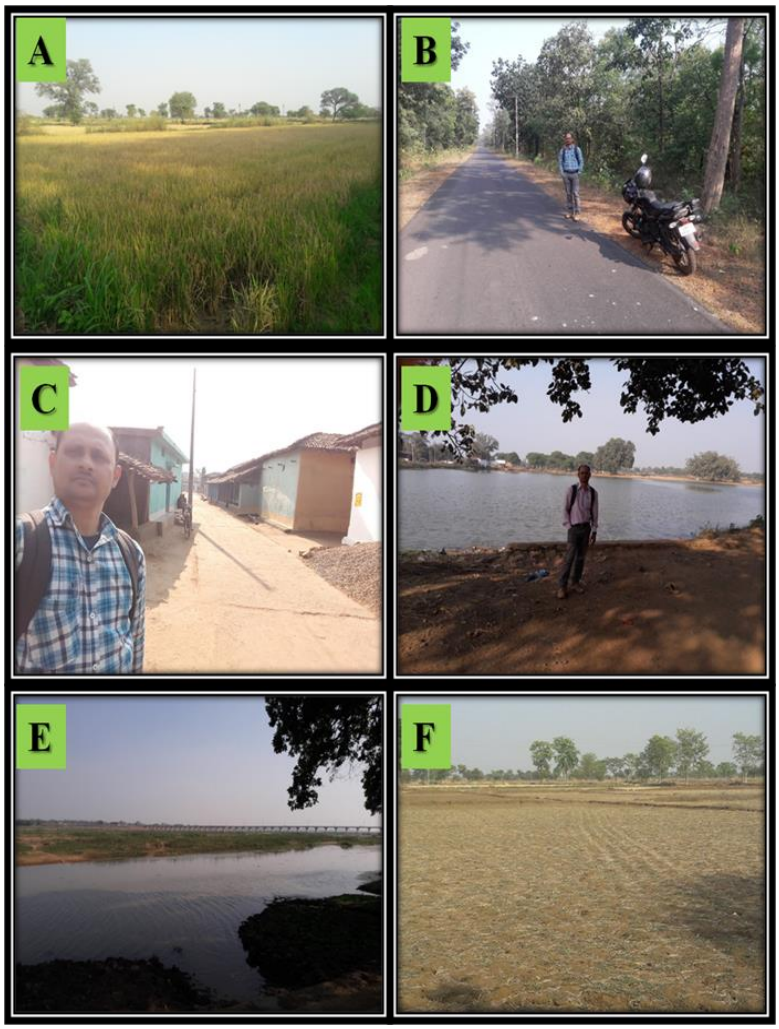

Insert Figure 5: Land Use Land Cover Classes of Study Area A) Paddy Crop, B) Forest, C) Settlement, D) Waterbody, E) Dry River and F) Uncultivated land.

2.10 Estimation of Agriculture Residues Based Bioenergy Potential

Zonal statistics tool was used for the estimation of village wise class of Paddy crop (major agriculture residue) in *Kharif* season as well as *Rabi* season in study area which was divided into 116 village boundaries. Study area vector boundary was used as input feature and reclassified paddy crop class was used as input raster to calculate village wise pixel count and area for bio-energy potential estimation in Kharif season for. Standard conversion was followed for the estimation of Paddy crop residues based bio-energy (MJ) using equations 3.

$$\mathbf{B_{ep}\,(Kharif) = C_c \times P_a \times C_p \times R_c \times S_r \times C_v} \quad \text{……..Eq. 3}$$

Where

B_{ep} (*Kharif*) = Bioenergy potential of paddy crop (MJ per annum)
C_c = Pixel count of particular crop class
P_a = Area of pixel (Hectare)
C_p = Average productivity of crop over 5 years (Quintal per hectare)
R_c = Crop to residue ratio [28,03]
S_r = Surplus crop residues available for bioenergy generation after fulfilling all domestic and farm requirements (50%) [09]
C_v = Calorific value (Low heating value) of crop (MJ/Quintal) [27,09]

Similar process was repeated for *Rabi* season crop to estimate bioenergy potential as B_{ep} (*Rabi*). Using bioenergy potential of *Kharif* season and bioenergy potential for *Rabi* season, annual bioenergy potential for the study area was calculated by equation 4.

$$\mathbf{B_{ep}\,(Annual) = \Sigma\, B_{ep}\,(Kharif) + B_{ep}\,(Rabi)} \quad \text{…….Eq. 4}$$

Where

B_{ep} (Annual) = Annual bioenergy generation potential over the study area (MJ)
B_{ep} (*Kharif*) = *Kharif* bioenergy generation potential over the study area (MJ)
B_{ep} (*Rabi*) = *Rabi* bioenergy generation potential over the study area (MJ)

At last village wise conversion table was prepared and linked to the shape files of village boundaries of block for GIS based depiction of agriculture biomass based bioenergy potential.

Estimation of Agriculture Based Bioenergy Potential Per Household

The total number of household in Magarlod is 24884 (Census, 2011). Village wise household quantity of bioenergy generation potential, estimated from the locally available bioresource *viz.,* agriculture residues (Paddy Straw) was used for further calculation of bioenergy potential per households with the following equations 5.

$$\mathbf{B_{ph} = B_{ep}(Annual) / H_v} \quad \text{……Eq. 5}$$

Where

B_{ph} = Agriculture Straw based bioenergy potential per household (MJ/Household)
B_{ep} (Annual) = Annual agriculture straw based bioenergy generation potential (MJ/annum)
Hv = Village wise number of household as per Census, 2011.

Estimation of Agriculture Based Bioenergy Potential Per Capita
The total population in Magarlod is 115150 distributed over 116 villages (Census, 2011). Village wise population with the bioenergy generation potential estimated from the locally available agriculture residues bioresource *viz.,* paddy straw was used the further calculation of bioenergy potential per capita village wise with the following equations 6.

$$\mathbf{B_{pc} = B_{ep}(Annual) / P_v} \quad \text{.....Eq. 6}$$

Where

B_{pc} = Agriculture Straw based bioenergy potential per capita (MJ/Household)
B_{ep}(Annual) = Annual agriculture straw based bioenergy generation potential (MJ/annum)
P_v = Village wise population as per Census, 2011

2.11. Confusion Matrix and Accuracy Assessment

Accuracy assessment is the most important step of any image classification process [23]. In fact it is the quantification of mapping data to group classification conditions, useful in validation of algorithms involve in classification, in order to determine the level of error over the image. Confusion matrix also called error matrix was a mean to determine the level of error and accuracy of the classification [04]. There are many methods of accuracy assessments in remote sensing. In the present study overall accuracy and kappa coefficient was used to validate the level of accuracy of the image classification [20]. Here a set of random points was created in classified map and compared with the ground truth data in a confusion matrix with reference map. The analysis was used for the calculation of confusion matrix, overall accuracy and kappa coefficients. Detail flowchart of methodology as per figure 6.

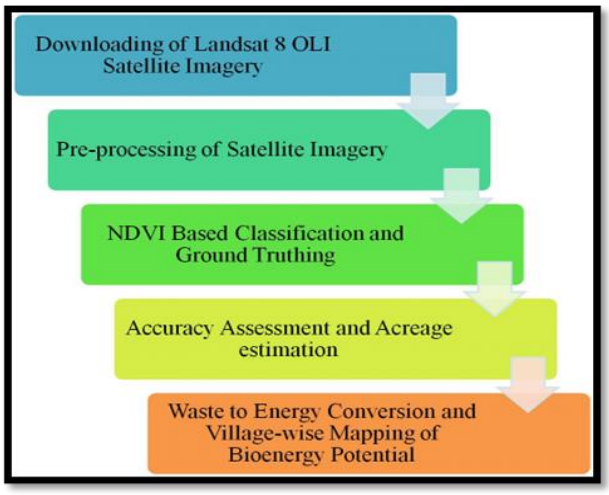

Insert Figure 6: Flowchart of Methodology

3.0 Results and Discussion

3.1. NDVI Analysis of Kharif Season Satellite Imagery:

The temporal analysis of the Landsat 8 OLI satellite image, illustrated the mean of the trends in alterations in vegetation using Normalized Difference Vegetation Indices (NDVI) in *Kharif* season (**Figure 7A**). The results shows the minimum, maximum, mean and range values of the time series satellite images of 2013, 2015 and 2016. The Kharif imagery of 2014 was not taken for study due to the heavy cloud cover over the entire season. The trends of mean imagery of minimum value were -0.09 and mean of maximum values was 0.32 while the mean range value was found as 0.41. The mean NDVI of temporal imagery of *Kharif* season was found as 0.20. The trends exhibited the consistent increase in mean value of NDVI showing increase in vegetation over the last three years of analysis in *Kharif* season (**Figure 8A, 8B & 8C**).

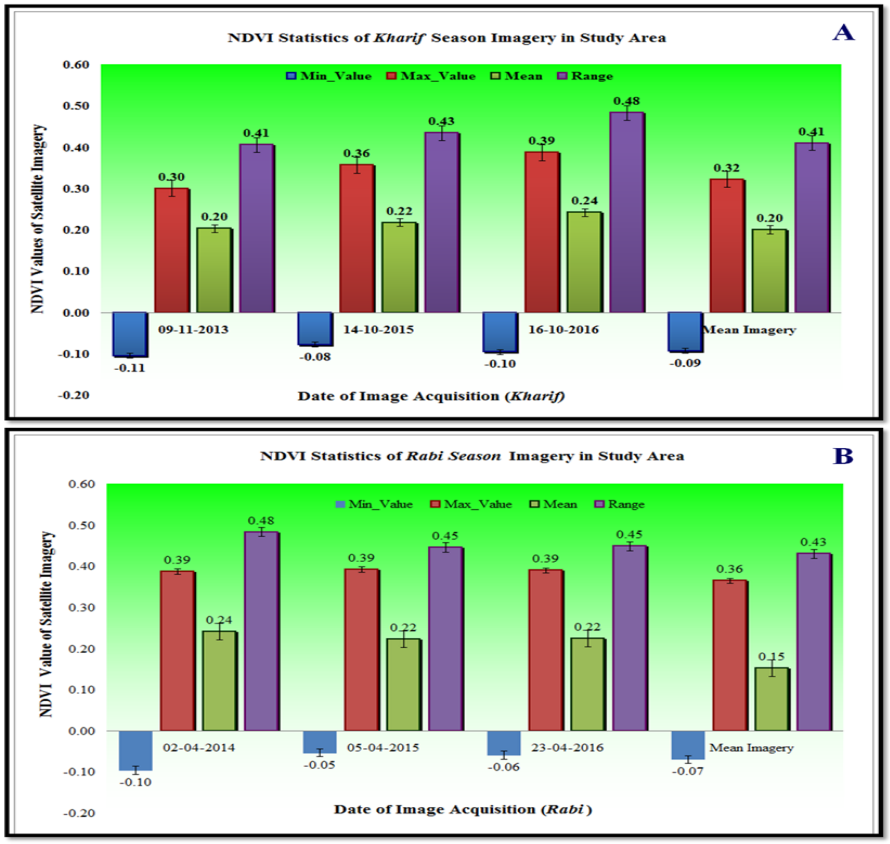

Insert Figure 7: NDVI statistics of Satellite Imagery in Study Area (A) Kharif Season and (B) Rabi Season.

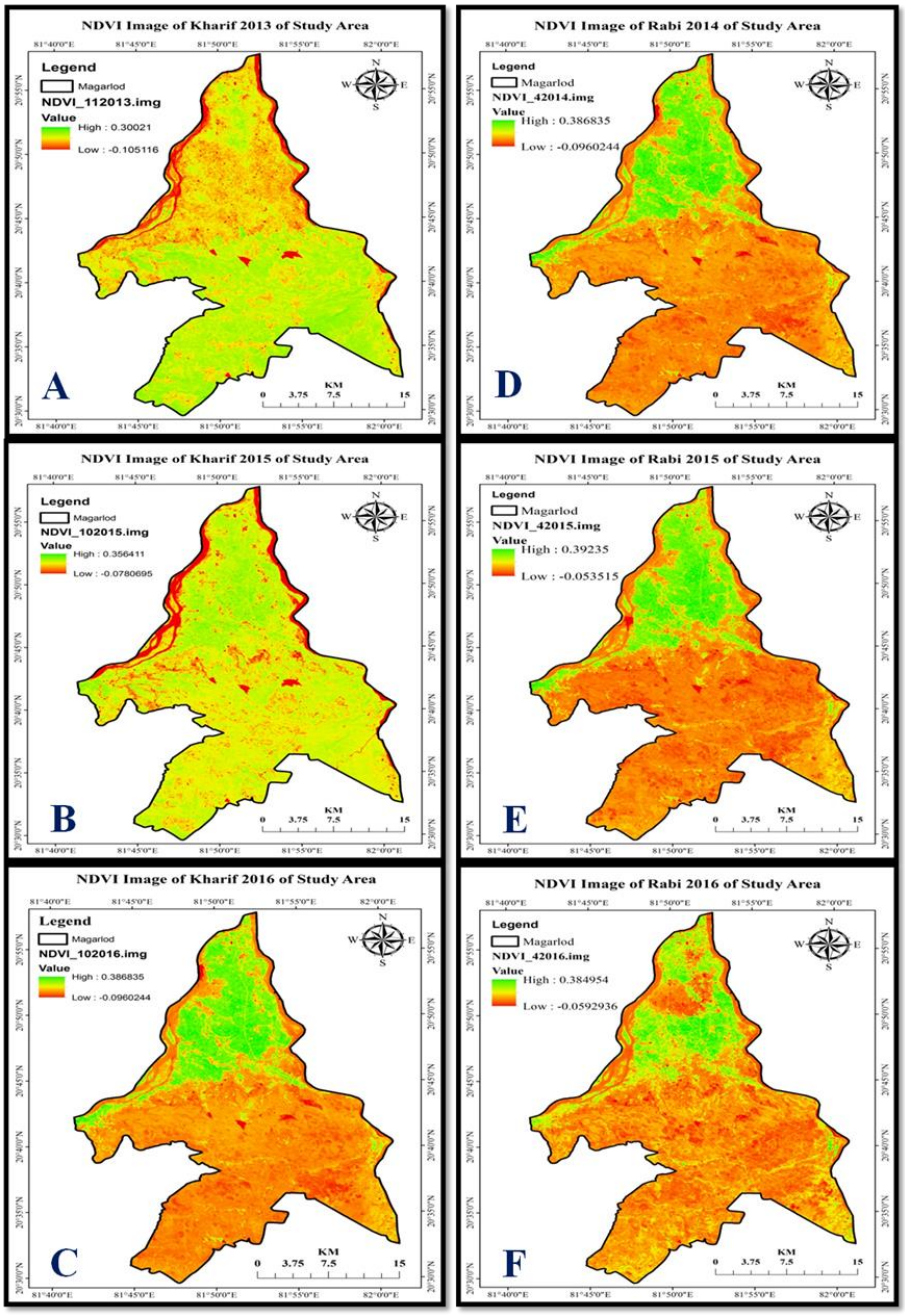

Insert Figure 8: Time series of NDVI for Kharif season (A) 2013, (B) 2015 & (C) 2016 and Rabi season (D) 2014, (E) 2015 & (F) 2016 of Study Area.

3.2. NDVI Analysis of Rabi Season Satellite Imagery

The temporal analysis of the Landsat 8 OLI satellite image, shows the mean of the trends in changes in vegetation using Normalized Difference Vegetation Indices (NDVI) in *Rabi* season (**Figure 7B**). The result shows the minimum, maximum, mean and range values of the time series satellite images of 2014, 2015 and 2016. The trends of mean of minimum value was -0.07 and mean of maximum values was 0.36 whereas mean range value was recorded as 0.43. The mean NDVI of temporal imagery of *Rabi* season was evidenced as 0.15. The trends revealed slightly decrease in mean value of NDVI showing deduction in vegetation over the last three years of analysis in *Rabi* season (**Figure 8D, 8E & 8F**). The mean NDVI image was reclassified to estimate the area of land use land cover classes (**Figure 9**). The results of the analysis show that area of the waterbody, dry river, settlement, uncultivated land, forest and paddy crop area was estimated to be 1559.2, 3433.1, 6822.0, 9094.1, 31640.5 and 25102.9 hectares in *Kharif* season whereas 1309.3, 3663.5, 6860.0, 20120.0, 31170.3 and 14527.9 hectares in *rabi* season respectively. The total pixel counts was 862798.0 and calculated area was 77651.8 hectares in study area (**Table 3**).

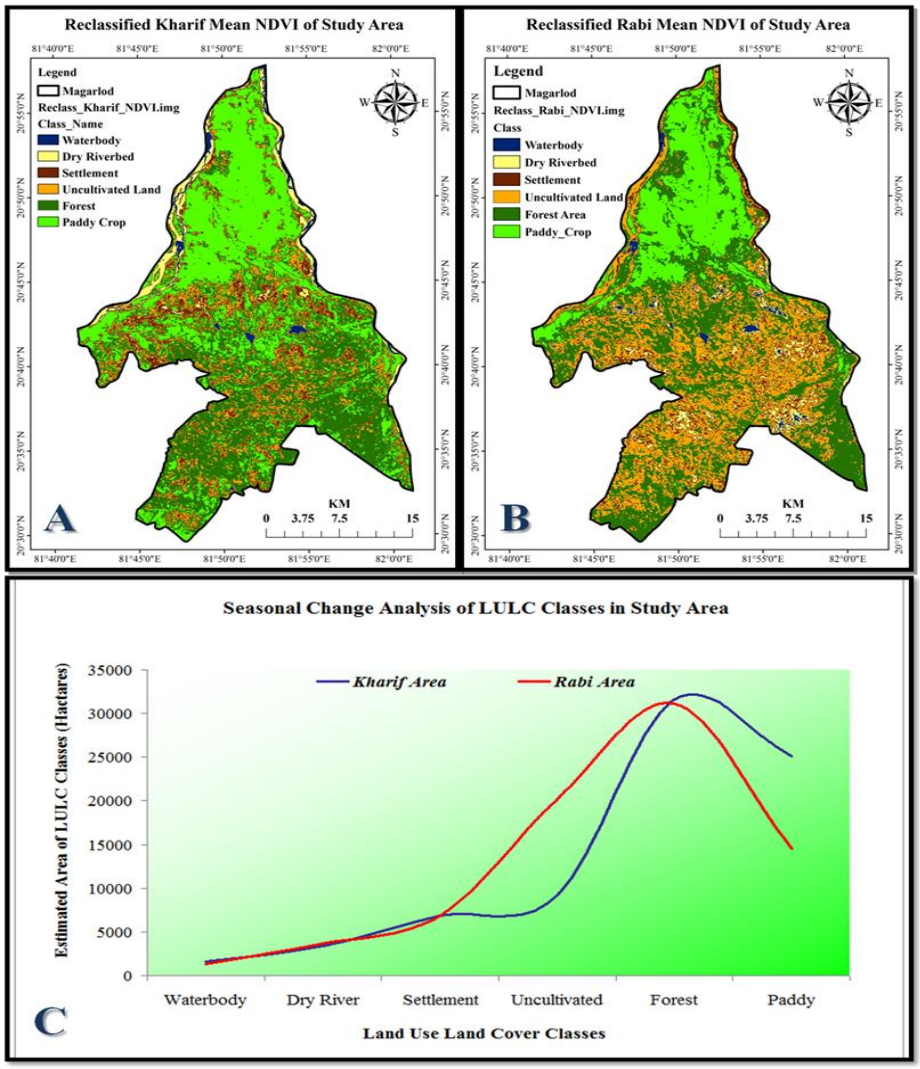

Insert Figure 9: Reclassified image of mean NDVI in (A) Kharif season and (B) Rabi season and (C) Seasonal change analysis of LULC classes in Study Area

Insert Table 3: Distribution of Estimated Area of Major Land Use Land Cover Classes in Mean NDVI Imagery of Kharif (A) and Rabi (B) in Study Area.

Code	Class	Kharif		Pixel Count	Area	Rabi		Pixel Count	Area
		Min	Max		Hectare	Min	Max		Hectare
1	Waterbody	-0.09	0.09	17324.0	1559.2	-0.07	0.09	14548.0	1309.3
2	Dry River	0.09	0.13	38146.0	3433.1	0.09	0.10	40706.0	3663.5
3	Settlement	0.13	0.17	75800.0	6822.0	0.10	0.11	76222.0	6860.0
4	Uncultivated	0.17	0.18	101046.0	9094.1	0.11	0.12	223564.0	20120.8
5	Forest	0.18	0.21	351561.0	31640.5	0.12	0.22	346337	31170.3
6	Paddy	0.21	0.32	278921.0	25102.9	0.22	0.36	161421	14527.9
Total		**Kharif**		**862798.0**	**77651.8**	**Rabi**		**862798.0**	**77651.8**

3.3. Change Analysis in Reclassified *Kharif* and *Rabi* Season:
The results of the change analysis of LULC classes of reclassified image of *Kharif* and *Rabi* season was shown in the figure 9C. It clearly shows that water body, forest and paddy crop have decreasing trends whereas dry river, settlements and uncultivated land have shown increasing trends. Major downfall was noted in the paddy crop area in *Rabi* season due to lack of irrigation and water resources facility in the study area.

3.4. Zonal availability of *Kharif* and *Rabi* Season Paddy Crop:
After the reclassification of the mean NDVI, the image was subjected to extraction of interested paddy crop area as was to find the area so as to estimate the agriculture particularly paddy straw based bioenergy potential in the study area. For this a single major class of paddy was extracted from all others major LULC classes from mean of temporal images of NDVI in *Kharif* and *Rabi* season. The pixel was counted and accordingly areas of paddy crop were estimated. It was found to be 25102.89 hectares in *Kharif* and 14527.89 hectares in *Rabi* season (**Figure 10A & 10B**). The data estimated from Landsat OLI 8 image based analysis was different from the district agriculture statistics. The difference was found to be less of 404.80 hectares in *Kharif* and about 677.89 hectares in *Rabi* season. The reasons of difference were delay in government report publication for the year, and record up gradation of new area under cultivation with increase in irrigation facility. (**Figure 10C**).

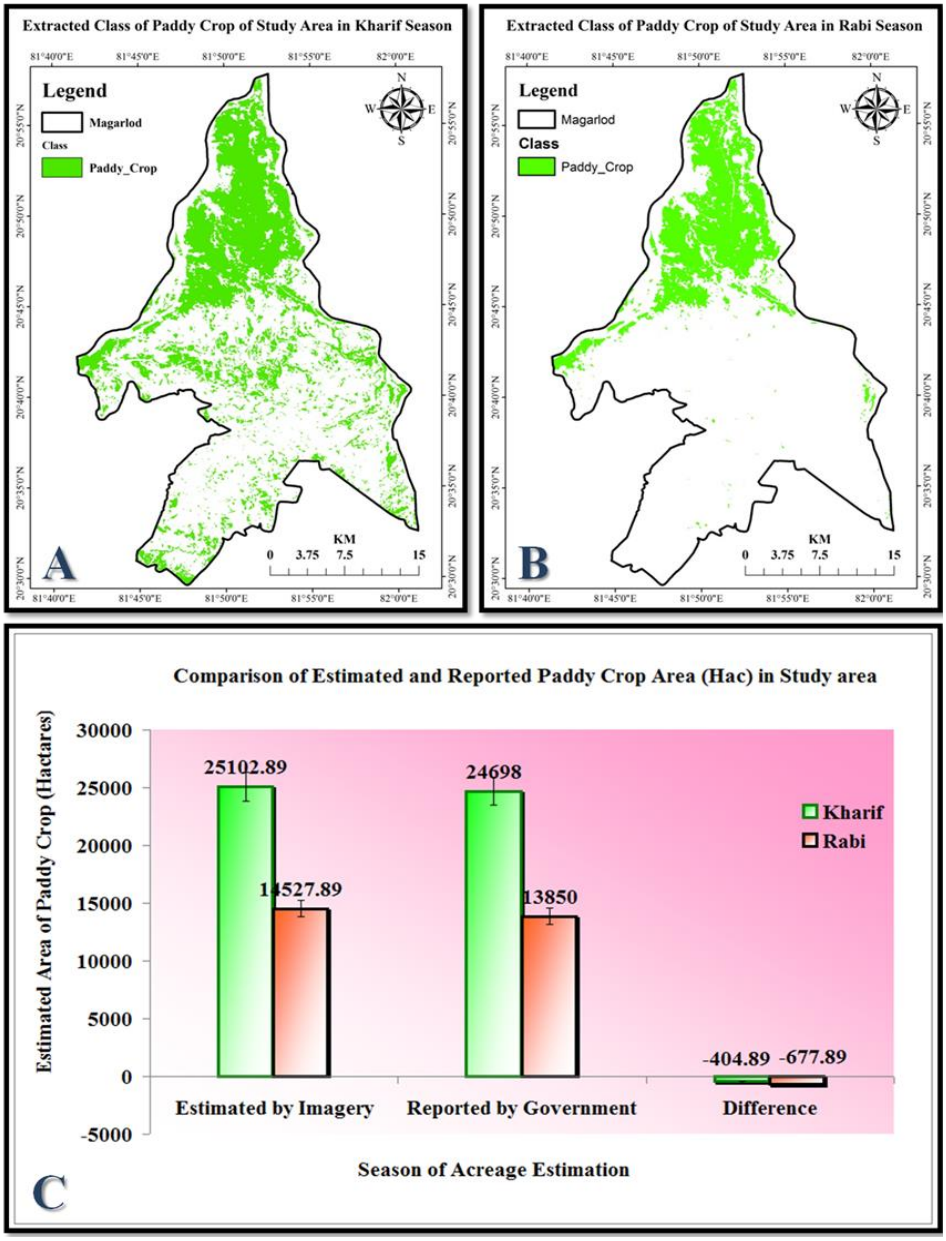

Insert Figure 10: Zonal availability of paddy crop in Kharif (A) and Rabi (B) Season and Comparative acreage gap analysis with government report of study area (C).

3.5. Zonal Estimation of Annual Surplus Paddy Straw Potential

Based on the estimated paddy area in *Kharif* and *Rabi* season, paddy production was estimation using last five year average productivity as 16.36 quintal per hectare reference from district statistics book 2013 of Dhamtari district with crop to residues ratio of 1.20. This was estimated separately for both the season and final straw production was summed up an annual straw production. As straw was meant for various purposes like manures, thatches, hut cover as well as bedding and feeding for livestock, an average of 50 per cent of estimated straw production only was taken as surplus straw available for bioenergy generation. The final map was generated village wise using number of pixel counts within the paddy class over the village boundary of study area. Here, forest villages were not taken into consideration as the area of villages are not registered in land revenue and other records in the name of farmers and all the land are the property of forest department of the government. The zonal statistics of the village wise straw was estimated in tonnes and were scaled in ten classes with equal interval for ease of map representation (**Figure 11**). The map shows that 73 villages falls under scale 1 having straw potential of 0-200 tonnes per annum, similarly 17 villages in scale 2 with 200-400 tonnes, 9 in scale 3 with 400-600 tonnes, 8 villages in scale 4 with 600-800 tonnes straw potential, 2 in scale 5 with 800-1000 tonnes, 2 in scale 6 with 1000-1200 tonnes, 1 village in scale 7 with 1200-1400 tonnes, 3 in scale 8 with 1400-1600 tonnes and 2 villages namely Khishora and Hasda were found in scale 10 with greater than 1800 tonnes of annual straw production. No villages were found under scale 9 with 1600-1800 tonnes of straw potential.

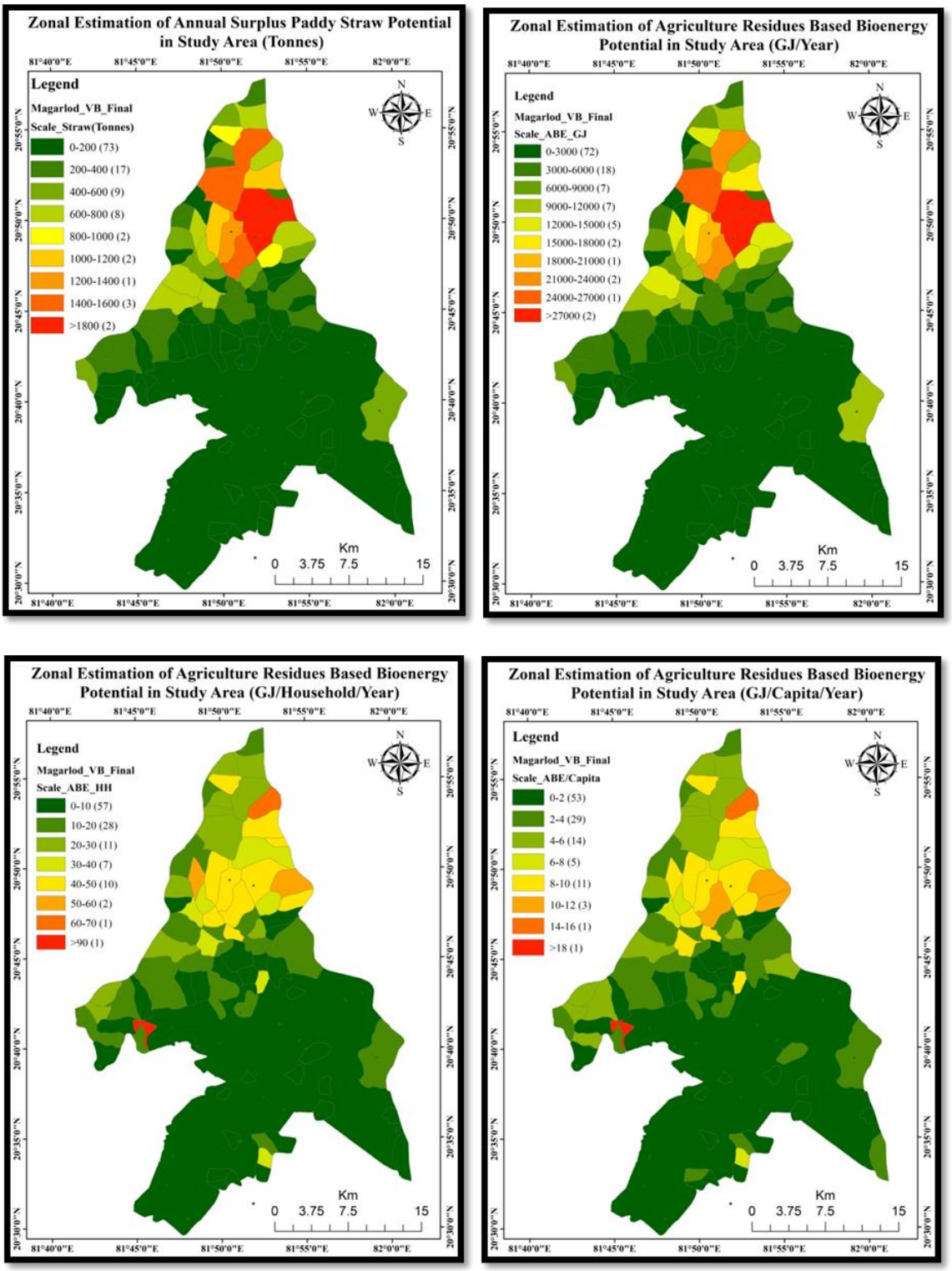

Insert Figure 11: Zonal Estimation of A) Annual Paddy Straw Potential, B) Annual Bioenergy Potential, C) Annual Bioenergy Potential per Household and D) Annual Bioenergy Potential per Capita in Study Area

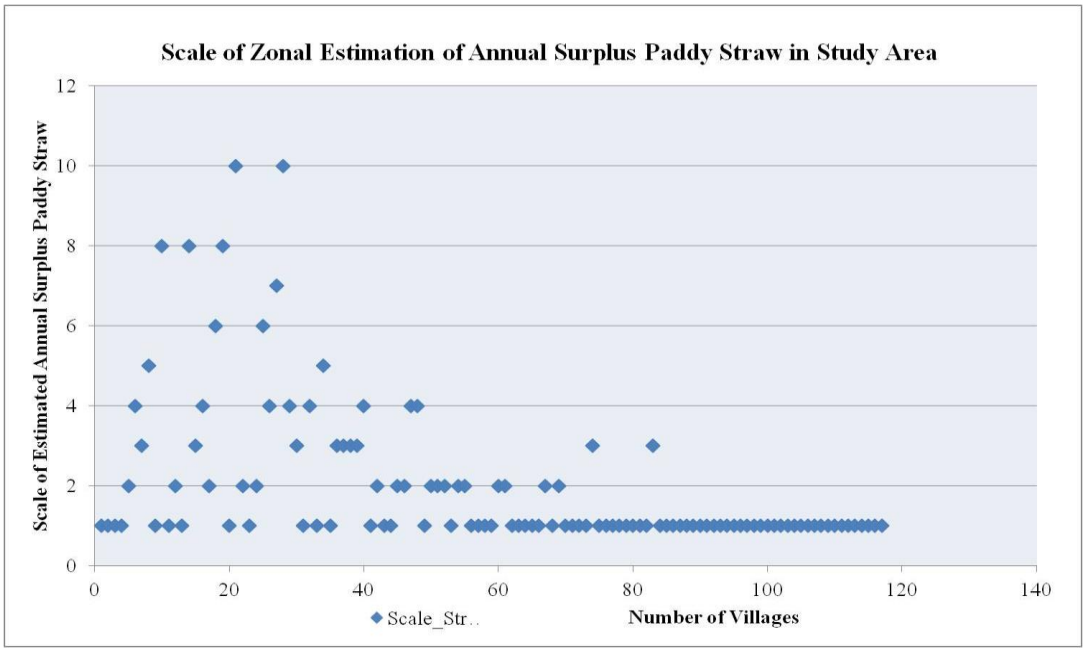

Insert Figure 12: Zonal Estimation of Annual Surplus Paddy Straw in Study Area

3.6. Estimation of Agriculture Residues Based Bioenergy Potential

The results of the estimation and scaling on 10 for annul agriculture residues based bioenergy potential village wise show that 72 villages fall in scale 1 with 0-3000 GJ of bioenergy followed by 18 villages in scale 2 with 3000-6000 GJ, 7 villages in scale 3 with 6000-9000 GJ of bioenergy, 7 villages in scale 4 with 9000-12000 GJ of bioenergy potential, 5 villages in scale 5 with 12000-15000 GJ, 2 villages namely Kundel and Mohrenga fall in scale 6 with 15000-18000 GJ, 1 village named Rakadih fall in scale 7 with 18000-21000 GJ, 2 villages that are Bhendri and Bhothidih fall in scale 8 with 21000-24000 GJ, one village that was Badi Kareli comes under scale 9 with 24000-27000 GJ of bioenergy and 2 villages namely Hasda and Khishora in scale 10 was having maximum potential with more than 27000 GJ of agriculture residue of paddy straw based bioenergy potential (**Figure 11B**).

3.7 Analysis of Agriculture Residues Based Bioenergy Potential per Household

The results of the analysis (**Figure 11C**) for the zonal estimation of agriculture residues based bioenergy potential per household per annum shows that over the ten scale, 57 villages comes under scale 1 within range of 0-10 GJ per household, followed by 28 villages fall under scale 2 within range of 10-20 GJ of bioenergy, similarly 11 villages fall in scale 3 with bioenergy range of 20-30 GJ, 7 villages in scale 4 within range of 30-40 GJ, 10 villages in scale 5 within range of 40-50 GJ bioenergy further 2 villages namely Belodi and Dumarpali comes under scale 6 within range of 50-60 GJ bioenergy, one village namely Parewadih comes under scale 7 within range of 60-70 GJ bioenergy and one village named Kewradih falls under scale 10 within range of bioenergy greater than 90 GJ bioenergy potential per household per annum. Among them Kewradih village shows the maximum bioenergy potential of 101 GJ per households per annum.

3.8 Analysis of Agriculture Residues Based Bioenergy Potential Per Capita

The results of the analysis (**Figure 11D**) for the zonal estimation of agriculture residues based bioenergy potential per capita per annum was shown over the ten scale, 53 villages comes under scale 1 within range of 0-2 GJ per capita, followed by 29 villages fall under scale 2 within range of 2-4 GJ of bioenergy similarly 14 villages fall in scale 3 with bioenergy range of 4-6 GJ, 5 villages in scale 4 within range of 6-8 GJ, 11 villages in scale 5 within range of 8-10 GJ bioenergy, further 3 villages namely Bhothidih, Dumarpali and Nardha come under scale 6 within range of 10-12 GJ bioenergy, next 1 village namely Parewadih comes under scale 8 within range of 14-16 GJ bioenergy and last 1 village named Kewradih falls under scale 10 within range of bioenergy greater than 18 GJ bioenergy potential per household per annum. Among them Kewradih village shows the maximum bioenergy potential of 20 GJ per capita per annum.

Statistical Analysis

3.9. Confusion Matrix and Accuracy Assessment

Assessment of accuracy is of utmost important for the understanding the levels of error in the analysis of land use land cover classes as well as target class. The confusion matrix was prepared after ground truthing in the *Kharif* season (Table 4). Furthermore, the result of the analysis of accuracy assessment for *Kharif* NDVI Classes of study area in table 4 shows class wise user's accuracy, producer accuracy, error of commission and error of omission. The overall accuracy was calculated to be 80.0 per cent whereas Kappa coefficient for Kharif NDVI accuracy assessment was 0.747. The result of the analysis of accuracy assessment for *Rabi* NDVI Classes of study area in table 5 shows class wise user's accuracy, producer accuracy, error of commission and error of omission. The overall accuracy was calculated to be 84.3 per cent whereas Kappa coefficient for *Rabi* NDVI accuracy assessment was 0.802. This results of the overall accuracy and kappa coefficient significantly shows the acceptability of the classification using NDVI in Landsat 8 OLI Satellite data.

Insert Table 4: Confusion Matrix of *Kharif* and *Rabi* NDVI of Study Area.

Reference	Code	Class	Waterbody	Dry River	Settlement	Uncultivated	Forest	Paddy	Total
Classified_Kharif	1	Waterbody	3	1	0	0	0	0	**4**
	2	Dry River	0	7	1	0	0	0	**8**
	3	Settlement	0	0	10	0	0	0	**10**
	4	Uncultivated	0	0	1	4	1	0	**6**
	5	Forest	1	0	0	1	7	0	**9**

	6	Paddy	0	0	0	0	6	17	**23**
		Total	**4**	**8**	**12**	**5**	**14**	**17**	**60**
Classified_Rabi	1	Waterbody	3	0	0	0	0	0	**3**
	2	Dry River	0	4	1	0	0	0	**5**
	3	Settlement	0	0	6	1	0	0	**7**
	4	Uncultivated	0	0	0	8	1	0	**9**
	5	Forest	0	0	0	1	8	1	**10**
	6	Paddy	0	0	0	1	2	14	**17**
		Total	**3**	**4**	**7**	**11**	**11**	**15**	**51**

Insert Table 5: Accuracy Assessment of *Kharif* NDVI and *Rabi* NDVI Classes.

S.No	Parameters	Waterbody	Dry River	Settlement	Uncultivated	Forest	Paddy
	Kharif						
1	Users Accuracy	75	87.5	83.33	80	50	100
2	Commission Error	25	12.5	16.67	20	50	0
3	Producers Accuracy	75	87.5	100	66.67	77.78	73.91
4	Omission Error	25	12.5	0	33.33	22.22	26.09
	Overall Accuracy	**80**			**Kappa Coefficient**	**0.747**	74.8
	Rabi						
1	Users Accuracy	100	100	85.71	72.73	72.73	93.33
2	Commission Error	0	0	14.29	27.27	27.27	6.67
3	Producers Accuracy	100	80	85.71	88.89	80	82.35
4	Omission Error	0	20	14.29	11.11	20	17.65
	Overall Accuracy	**84.3**			**Kappa Coefficient**	**0.8**	80.2

Discussions

The results of the LULC change analysis on the area of the major classes of *Kharif* and *Rabi* reclassified image clearly shows that water body, forest and paddy crop have decreasing trends whereas dry river, settlements and uncultivated land have shown increasing trends. Major downfall has been shown in the paddy crop area due to lack of irrigation and water resources facility in the study area. After the reclassification of the mean NDVI, the image was subjected to extraction of interested paddy crop area as our aim was to find the area so as to estimate the agriculture particularly paddy straw based bioenergy potential in the study area. For this a single major class of paddy was extracted from all others major LULC classes from mean of temporal images of NDVI in *Kharif* and *Rabi* season. The pixel was counted and accordingly areas of paddy crop were estimated. It was found to be 25102.89 hectares in *Kharif* and 14527.89 hectares in *Rabi* season. The data estimated from Landsat OLI 8 Image based analysis was different from the district agriculture statistics. The difference was found to be less of 404.80 hectares in *Kharif* and about 677.89 hectares in *Rabi* season. One of the simplest uses of remote sensing for agricultural activities is to create maps of the agro-ecological setting. It may be constructive to remind the difference between land cover, which relates to the physical characteristics of a land surface, and land use, which corresponds to the functions for which humans use the land [18].

On the other hand, conventionally, rustic areas have been linked with the demand-side of energy systems, ensuing from their extensive supplies for energy services and the physical and communal constraints. Conversely, rising opportunities for small-scale distributed energy production technologies within the rural society [16]. Further, the promotion of constructional energy efficiency and support for communal energy systems has amplified the function and liability of local governments and organizations for supervision and planning associated to energy [15,05]. Although, the present study clarified that straw was meant for various purposes like manures, thatches, hut cover as well as bedding and feeding for livestock, an average of 50 % was only taken as surplus straw available for bioenergy potential. Further, the straw production estimated separately for both *Kharif* and *Rabi* season and a final straw production was added to analyze annual straw production. The zonal statistics of the village wise straw was estimated in tonnes and were scaled in ten classes with equal interval for ease of map representation. The map shows that 73 villages falls under scale 1 having straw potential of 0-200 tonnes per annum, similarly 17 in scale 2 with 200-400 tonnes, 9 in scale 3 with 400-600 tonnes, 8 villages in scale 4 with 600-800 tonnes straw potential, 2 in scale 5 with 800-1000 tonnes, 2 in scale 6 with 1000-1200 tonnes, 1 village in scale 7 with 1200-1400 tonnes, 3 in scale 8 with 1400-1600 tonnes and 2 villages namely Khishora and Hasda were found in scale 10 with greater than 1800 tonnes of annual straw production. No villages were found under scale 9 with 1600-1800 tonnes of straw potential.

4.0 Summary and Conclusions

The agricultural residues potentiality of study area was estimated through Remote Sensing and GIS applications. Consequently, the temporal analysis of the Landsat 8 OLI satellite image shows the mean of the trends in changes in vegetation using Normalized Difference Vegetation Indices (NDVI) in *Kharif* and *Rabi* season. The results for *Kharif* season was founded as 0.20 whereas mean of range was founded as 0.43 for *Rabi* season. The mean of temporal imagery of Rabi season was founded as 0.15. The trends shows the slightly decrease in mean value of NDVI showing deduction in vegetation over the last three years of analysis in Rabi season. The mean NDVI image was reclassified to estimate the area of land use land cover classes. The results of the analysis shows that area of the waterbody, dry river, settlement, uncultivated land, forest and paddy crop area was estimated to be 1559.2, 3433.1, 6822.0, 9094.1, 31640.5 and 25102.9 hectares in Kharif season whereas 1309.3, 3663.5, 6860.0, 20120.0, 31170.3 and 14527.9 hectares in Rabi season. Total pixel counts were estimated to be 862798.0 and area to be 77651.8 hectares in both the season of study area and accordingly areas of paddy crop were estimated. It was found to be 25102.89 hectares in *Kharif* and 14527.89 hectares in *Rabi* season. The data estimated from Landsat OLI 8 image based analysis was different from the district agriculture statistics. The difference was found to be less of 404.80 hectares in *Kharif* and about 677.89 hectares in *Rabi* season. Assessment of accuracy is of utmost important for the understanding the levels of error in the analysis of land use land

cover classes as well as target class. The confusion was prepared after the ground truthing in *Kharif* season. Furthermore, the result of the analysis of accuracy assessment for *Kharif NDVI* Classes of study area shows class wise user's accuracy, producer accuracy, error of commission and error of omission. The overall accuracy was calculated to be 80.0 per cent whereas Kappa coefficient for *Kharif* NDVI accuracy assessment was 0.747. The result of the analysis of accuracy assessment for *Rabi* NDVI Classes of study area shows class wise user's accuracy, producer accuracy, error of commission and error of omission. The overall accuracy was calculated to be 84.3 per cent whereas Kappa coefficient for *Rabi* NDVI accuracy assessment was 0.802. This results of the overall accuracy and kappa coefficient significantly shows the acceptability of the classification using NDVI in Landsat 8 OLI Satellite imagery.

Acknowledgement and Financial Assistance

I would like to thank Head, Department of Rural Technology and Social Development, Guru Ghasidas Vishwavidyalaya, Bilaspur, Chhattisgarh for providing me an opportunity to work and necessary resources and support providing for carrying out this study.

Conflict of Interest

None

References

[1] Aselmann I, and Crutzen P.J. (1989). Global distribution of natural freshwater wetlands and rice paddies their net primary productivity seasonality and possible methane emissions J Atmos Chem 8: 307-358.

[2] Avtar, R., Sahu, N., Agarwal, A. K., Chakraborty, S., Kharrazi, A., Yunus, A. P. and Kurniawan, T. A. (2019). Exploring renewable energy resources using remote sensing and GIS—A review. *Resources*, **8(3)**, 149.

[3] BRAI-Biomass Resource Atlas of India. CGPL: Indian Institute of Science, Bangalore. http://lab.cgpl.iisc.ernet.in/Atlas/ 2009.

[4] Congalton, R. G. (1991). A review of assessing the accuracy of classifications of remotely sensed data. *Remote sensing of environment*, **37(1)**: 35-46.

[5] Denis, G.S. and Parker, P. (2009). Community energy planning in Canada: The role of renewable energy. *Renewable and Sustainable Energy Reviews*, **13**: 2088–2095.

[6] Egbert S.L, Park S, Price K.P. (2002) Using conservation reserve program maps derived from satellite imagery to characterize landscape structure. Comput Electron Agric 37: 141-56.

[7] Foody, G. M. and Mathur, A. (2004). Toward intelligent training of supervised image classifications: directing training data acquisition for SVM classification. *Remote Sensing of Environment*, **93(1-2)**: 107-117.

[8] Frolking S. (2002) Combining remote sensing and ground census data to develop new maps of the distribution of rice agriculture in China Glob Biogeochem Cycles16: 1091.

[9] Hiloidhari, M. and Baruah, D. C. (2011). Rice straw residue biomass potential for decentralized electricity generation: a GIS based study in Lakhimpur district of Assam, India. *Energy for Sustainable Development*, **15(3)**: 214-222.

[10] Holden, C. E., & Woodcock, C. E. (2016). An analysis of Landsat 7 and Landsat 8 underflight data and the implications for time series investigations. *Remote Sensing of Environment*, *185*, 16-36.

[11] http://censusindia.gov.in/2011census/Part_A_Dhamtari.pdf

[12] https://censusindia.gov.in/2011census/Part_B_Dhamtari.pdf

[13] https://eands.dacnet.nic.in/PDF/Agricultural_Statistics_At_Glance-2015.pdf

[14] https://earthexplorer.usgs.gov.

[15] Kavgic, M. (2010). A review of bottom-up building stock models for energy consumption in the residential sector. *Building and Environment*, **45**: 1683–1697.

[16] Keirstead, J. (2012). A review of urban energy system models: Approaches, challenges and opportunities. *Renewable and Sustainable Energy Reviews*, **16**: 3847–3866.

[17] Kusre, B. C., Baruah, D. C., Bordoloi, P. K. and Patra, S. C. (2010). *Applied Energy*, **87(1)**: 298-309.

[18] Lambin, E. F., Geist, H. and Rindfuss, R. R. (2006). Introduction: local processes with global impacts. In *Land-use and land-cover change*: pp. 1-8. Springer, Berlin, Heidelberg.

[19] Lehner, M., Tichler, R., Steinmüller, H. and Koppe, M. (2014). *Power-to-gas: technology and business models*. Springer.

[20] Lu, D., Mausel, P., Brondizio, E., & Moran, E. (2004). Change detection techniques. *International journal of remote sensing*, *25*(12), 2365-2401.

[21] Matthews E, Fung I, Lerner J (1991) Methane emission from rice cultivation Geographic and seasonal distribution of cultivated areas and emissions. Glob Biogeochem Cycles 5: 3-24.

[22] Nuarsa, I. W., Nishio, F., & Hongo, C. (2011). Spectral characteristics and mapping of rice plants using multi-temporal Landsat data. *Journal of Agricultural Science*, *3*(1), 54.

[23] Patil, M. B., Desai, C. G. and Umrikar, B. N. (2012). Image classification tool for land use/land cover analysis: A comparative study of maximum likelihood and minimum distance method. *Int J Geol Earth Environ Sci*, **2**: 189-196.

[24] Pocket Book of Agriculture Statistics. (2017). Department of Agriculture, Cooperation & Farmer's Welfare. Directorate of Economics & Statistics. New Delhi.

[25] Roy, D. P., Wulder, M. A., Loveland, T. R., Woodcock, C. E., Allen, R. G., Anderson, M. C., ... and Scambos, T. A. (2014). Landsat-8: Science and product vision for terrestrial global change research. *Remote sensing of Environment*, **145**: 154-172.

[26] Samanta, K. P. (2015). A Study of Rural Electrification Infrastructure in India. *IOSR Journal of Business and Management Ver. IV*, **17(2)**: 2319–7668.

[27] Singh, J., Panesar, B. S. and Sharma, S. K. (2008). Energy potential through agricultural biomass using geographical information system—A case study of Punjab. *Biomass and Bioenergy*, **32(4)**: 301-307.

[28] Singh, R. B., Saha, R. C., Singh, M., Chandra, D., Shukla, S. G., Walli, T. K. and Kessels, H. P. P. (1995). Rice straw, its production and utilization in India. In *Handbook for straw feeding systems in livestock production* ICAR. pp 325-339.

[29] Thenkabail P.S. (2012) Assessing Future Risks to Agricultural Productivity Water Resources and Food Security How Can Remote Sensing Help Photogram Eng Remote Sensing 78: 773-782.

[30] Tucker, C. J. (1979). Red and photographic infrared linear combinations for monitoring vegetation. *Remote sensing of Environment*, **8(2)**: 127-150.

[31] Vogelmann, J. E., Gallant, A. L., Shi, H., & Zhu, Z. (2016). Perspectives on monitoring gradual change across the

continuity of Landsat sensors using time-series data. *Remote Sensing of Environment*, *185*, 258-270.

[32] Wardlow, B. D., & Egbert, S. L. (2008). Large-area crop mapping using time-series MODIS 250 m NDVI data: An assessment for the US Central Great Plains. *Remote sensing of environment*, *112*(3), 1096-1116.

[33] Wulder, M. A., Bater, C. W., Coops, N. C., Hilker, T. and White, J. C. (2008). The role of LiDAR in sustainable forest management. *The Forestry Chronicle*, **84(6)**: 807-826.

CV of Author

Dr. Hemant Sahu - PhD Scholar, Department of Rural Technology and Social Development, Guru Ghasidas Vishwavidyalaya, Bilaspur Chhattisgarh. Email: info2hemant1980@gmail.com.

Dr. Pushpraj Singh - Associate Professor and Head, Department of Rural Technology and Social Development, Guru Ghasidas Vishwavidyalaya, Bilaspur Chhattisgarh. Email: contactprsingh@gmail.com.